[33]E. A. Stern and R. A. Ferrell, Phys. Rev. 120, 130 (1960).
[34]P. J. Feibelman, Phys. Rev. 176, 551 (1968).
[35]J. I. Gersten, Phys. Rev. 188, 774 (1969).
[36]P. J. Feibelman, Phys. Rev. (to be published).
[37]C. B. Duke, G. E. Laramore, B. W. Holland, and A. M. Gibbons, Surface Sci. (to be published).
[38]A. Bagchi, C. B. Duke, and P. J. Feibelman (unpublished).
[39]C. W. Tucker, Jr. and C. B. Duke, Surface Sci. 23, 411 (1970).
[40]C. B. Duke and C. W. Tucker, Jr., J. Vacuum Sci. Technol. 8, 5 (1971).
[41]W. D. Robertson, J. Vacuum Sci. Technol. 8, 3 (1971).
[42]J. M. Baker, Ph. D. thesis (Cornell University, 1970) (unpublished).
[43]Note that the position of the maxima in the theoretical curves in Fig. 2 of Ref. 1 do *not* agree with their positions shown in Fig. 1 of this reference. For example, in the $\theta = 10°$ profiles, the higher-energy component of the secondary-split Bragg peaks near 100 eV lies clearly above 100 eV in Fig. 1 but clearly below 100 eV in Fig. 2. From the discussion at the bottom of p. 518 in Ref. 1 we infer that in Fig. 1 (a) (unspecified) shift of all the profiles has been performed using the Lundquist self-energy to determine the value of this shift. Concerning Fig. 2, Jones informs us that drafting errors occurred in its construction, but we still are unable to reproduce its construction from Fig. 1.
[44]Substantial progress in this endeavor has been achieved since the submission of this manuscript. Results on Al(100) have been reported at the 1971 LEED Seminar by Marcus and Jepson, Tony and Rhodin, Strozier and Jones, and Duke, Laramore, and Tucker. Calculations on the nonspecular beams of Be(0001) were reported by Strozier and Jones and by Zimmer, and on Al(111) and Al(110) by Duke, Laramore, Holland, and Gibbons. These analyses reveal that using an improved electron-ion-core potential materially improves the description of data for small angles of incidence and intermediate energies ($20 \leq E \leq 200$ eV). The description of data at low energies and large ($\theta \gtrsim 15°$) angles of incidence remains qualitative in nature.
[45]C. B. Duke, A. J. Howsmon, and G. E. Laramore, J. Vacuum Sci. Technol. 8, 10 (1971).
[46]C. B. Duke, and C. W. Tucker, Jr. (unpublished).
[47]H. H. Farrell and G. A. Somorjai, Phys. Rev. 182, 751 (1969).
[48]F. Jona, IBM J. Res. Dev. 14, 444 (1970).
[49]P. M. Morse, Phys. Rev. 35, 1310 (1930).

PHYSICAL REVIEW B VOLUME 3, NUMBER 10 15 MAY 1971

Anharmonic Interactions in Aluminum. II

N. S. Gillis*
Sandia Laboratories, Albuquerque, New Mexico 87115
and
T. R. Koehler
IBM Research Laboratory, San Jose, California 95114
(Received 4 November 1970)

Additional calculations of the one-phonon spectral function in aluminum are presented. Results are given in the temperature range $300 \lesssim T \lesssim 900$ K for phonons propagating along the symmetry directions [100], [110], [111], and [310]. The frequency shifts and linewidths of the [310] phonons are compared with the high-temperature neutron scattering data of Larsson *et al.* In addition, for those phonons whose resonance shapes develop prominent structure, the spectral functions are explicitly displayed and discussed.

I. INTRODUCTION

In a previous paper[1] anharmonic linewidths and frequency shifts were calculated for aluminum at the two temperatures 80 and 300 K for phonons propagating along the [100], [110], and [111] symmetry directions. Agreement with the available experimental neutron scattering data was satisfactory. The calculation was based on a model pseudopotential whose parameters were determined so as to reproduce the experimental phonon dispersion curves in aluminum at 80 K.

The present work extends the calculations of I to higher temperatures. The approximations involved are the same as were discussed previously. In the treatment of I, only the lowest-order anharmonic corrections to the phonon self-energy were included, i.e., the quartic interaction to first order and the cubic interaction to second order. Since the Debye temperature of aluminum is ~ 400 K, we might expect that the neglect of anharmonic interactions of higher order (e.g., four-phonon decay processes) would introduce quantitative errors for $T \gg \Theta_D$. In order to obtain a partial assessment of the importance of the higher-order anharmonic corrections, calculations of frequency shifts and linewidths were carried out for selected [310] phonons and comparison made with the high-temperature neutron data of Larsson *et al.*[2] Satisfactory agreement was found for the over-all trends with temperature of the frequency shifts and linewidths over the range of temperatures considered. The large ex-

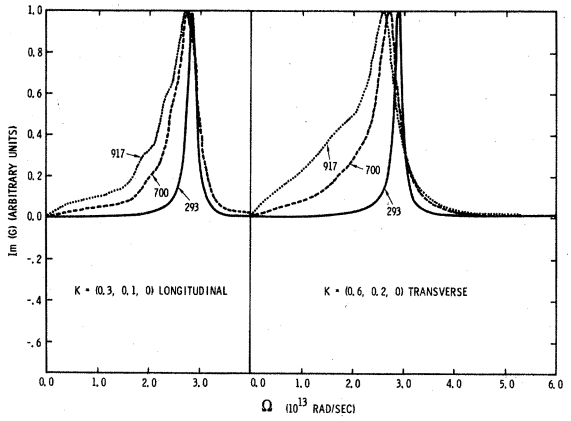

FIG. 1. One-phonon spectral function $\mathrm{Im}[G(\Omega)]$ plotted as a function of frequency at several temperatures for two phonons along the [310] direction. The curves are labeled with the value of the temperature (K), and K is the propagation vector.

perimental errors precluded any quantitative comparison between theory and experiment. However, the qualitative features of the experimental data were reproduced with enough success to motivate additional calculations at high temperatures employing only the lowest-order anharmonic theory. Furthermore, it was thought that the uncertainties already present in the higher-order spatial derivatives of the model potential did not justify pursuing a more sophisticated anharmonic approximation than that already employed in I.

In Sec. II we present the results of our calculations for selected [310] phonons in the temperature range $300 \lesssim T \lesssim 900$ K, together with the experimental data of Larsson *et al.* The remaining part of Sec. II is then concerned with a study of the shapes of the one-phonon spectral functions for the [100], [110], and [111] symmetry directions. A distinctive feature which arises from this study is the fact that the one-phonon resonance remains well defined for the majority of phonons along the major symmetry directions. We consider explicitly those phonons which develop prominent structure as the temperature is raised.

II. RESULTS

The one-phonon contribution to the neutron scattering cross section is proportional to

$$\sum_{\lambda,\lambda'} [\vec{q}\cdot\vec{e}(q,\lambda)][\vec{q}\cdot\vec{e}(q,\lambda')]\,\mathrm{Im}G_{\lambda\lambda'}(\vec{q},\omega+i0^{+}), \tag{1}$$

where $\vec{q}$ and ω are the momentum and energy transfer, respectively, $\vec{e}(q,\lambda)$ is the harmonic polarization vector associated with mode λ, and $G_{\lambda\lambda'}$ is the one-phonon Green's function. For the Δ, Λ, and Σ modes of a cubic crystal, $G_{\lambda\lambda'}$ is exactly diagonal. However, for directions other than the three principal symmetry directions, the off-diagonal elements of $G_{\lambda\lambda'}$ are, in general, nonzero. One must then perform an exact matrix solution of the appropriate Dyson equation in order to obtain the elements of $G_{\lambda\lambda'}$ for insertion in Eq. (1). Such a matrix solution was carried out for $\vec{q}$ directed along the [310] direction. With $\vec{q}$ so oriented, three independent terms contribute to Eq. (1)—two diagonal and one off-diagonal. For the two phonons of interest with propagation vectors (0.6, 0.2, 0) and (0.3, 0.1, 0), the off-diagonal contribution was found to be negligible over the whole range of temperatures considered. The diagonal contributions then give rise to a high-frequency and a low-frequency resonance which we denote by "longitudinal" and

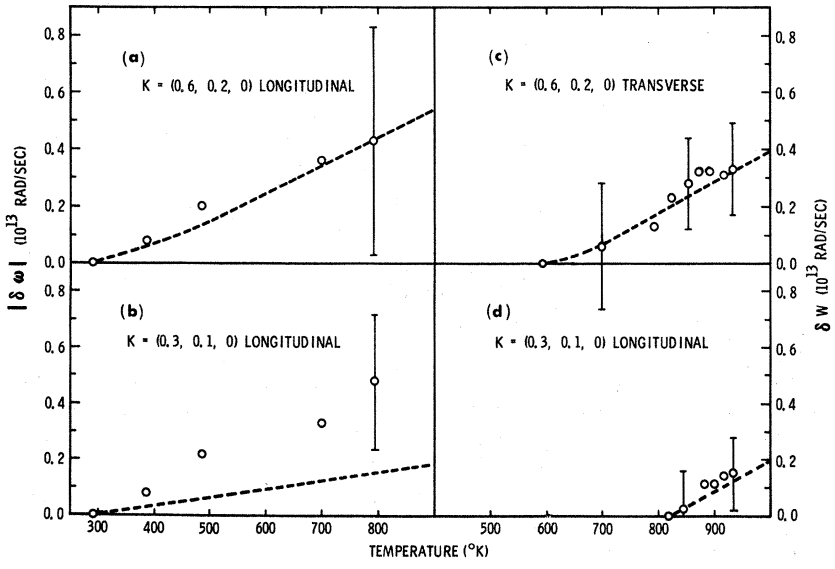

FIG. 2. (a) and (b) Decrease with temperature of the frequencies of selected phonons along the [310] direction, $|\delta\omega| \equiv \omega(300\ \mathrm{K}) - \omega(T)$. (c) Increase with temperature of the width of the (0.6, 0.2, 0) transverse phonon, $\delta\omega \equiv 2[\Gamma(T) - \Gamma(600\ \mathrm{K})]$. (d) Increase with temperature of the width of the (0.3, 0.1, 0) longitudinal phonon, $\delta\omega \equiv 2[\Gamma(T) - \Gamma(820\ \mathrm{K})]$. The experimental points are given by open circles; the dotted lines represent the theoretical prediction based on Eq. (2) of the text.

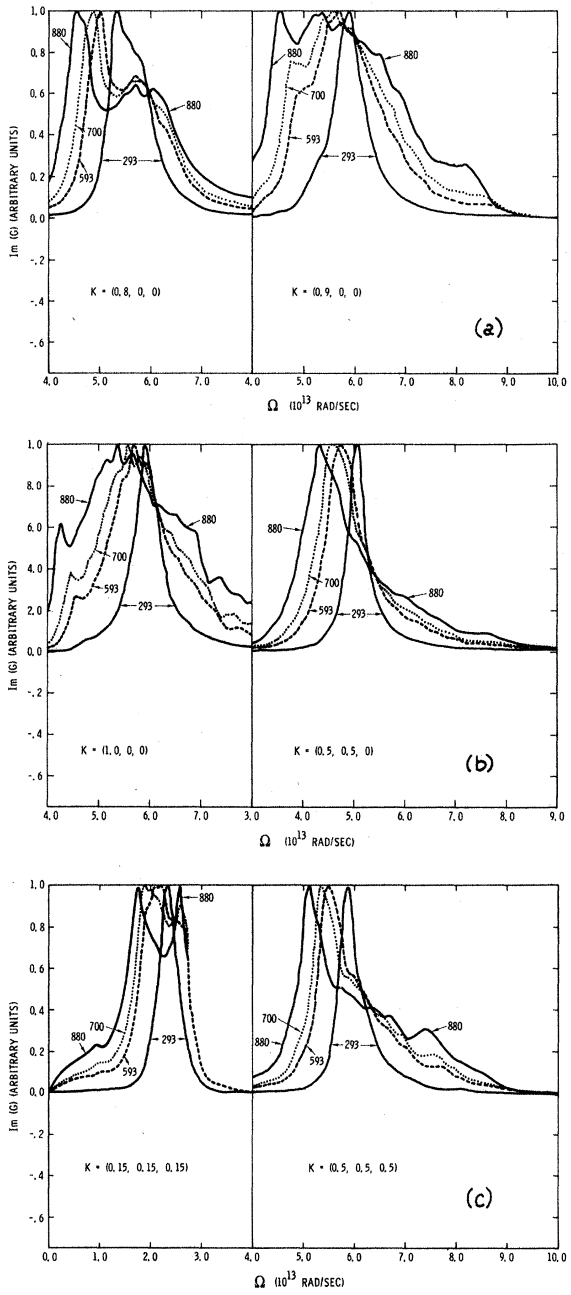

FIG. 3. (a)–(c) Same as Fig. 1 but for the three principal symmetry directions.

"transverse," respectively. Figures 1 and 2 give some representative results for the (0.6, 0.2, 0) and (0.3, 0.1, 0) phonons in the temperature range 300–900 K. Figure 1 depicts the shape of the one-phonon resonance at three representative temperatures; it is clear that the resonance remains well defined over the whole temperature range. Figure 2 plots results for the magnitude of the decrease in frequency with T as well as the increase with T of the resonance full width at half-maximum over the temperature range 300–900 K. The dotted curves are the theoretical predictions based on the approximations

$$\omega \approx \omega_0 + \Delta(\omega_0), \qquad W \approx 2\Gamma(\omega_0), \tag{2}$$

where ω_0 is the quasiharmonic frequency and $\Delta(\omega)$ and $\Gamma(\omega)$ are the real and imaginary parts of the phonon self-energy. Within the context of the anharmonic approximation employed in I, the high-temperature limit of the expressions in Eq. (2) yields the linear T dependence shown in Fig. 2. The difference between the true position of the resonance maxima and the position predicted by the approximation of Eq. (2) is negligible for the cases considered. However, the true widths of the theoretical one-phonon resonances differed somewhat from their approximate values given in Eq. (2). The agreement between experiment and theory for the (0.6, 0.2, 0) phonons is quite satisfactory, whereas the agreement for the (0.3, 0.1, 0) phonons is less satisfactory with the δ_ω-vs-T curve showing the worst agreement. It is striking, however, that the approximations of Eq. (2) work as well as they do over the large temperature range considered. This can be attributed in part to the slow frequency variation of $\Delta(\omega)$ and $\Gamma(\omega)$ in the region near the resonance maximum, as well as to the fact that the resonance maintains a quasi-Lorentzian structure up to the highest temperatures considered.

Figures 3(a)–3(c) depict the variation with temperature of frequency plots of the one-phonon spectral functions for selected longitudinal phonons along the principal symmetry directions. All remaining longitudinal phonons, as well as all transverse phonons, maintain an essentially Lorentzian structure over the complete range of temperatures considered. It is also of interest here to point out another qualitative feature which arose out of our study of the phonon line shapes. It was found that in the region near the zone boundary, the attenuation of longitudianl phonons was a factor of 5–10 greater than that for transverse phonons. Qualitatively, this behavior can be understood in terms of energy-momentum-conservation conditions for high-frequency phonons[3] satisfying $\hbar\omega > k_B T$ (this inequality is satisfied in the present case at the zone boundary even for $T \sim 900$ K). Furthermore, it was found that the opposite limiting case $\hbar\omega < kT$ exhibited qualitative behavior consistent with the Landau-Rumer prediction, i.e., that the attenuation of the transverse phonons exceeds that of the longitudinal phonons.

The (0.8, 0, 0) longitudinal mode is the only mode exhibiting an asymmetric resonance shape at room temperature; as was explained in I, this asymme-

try can be ascribed to the decay process $\omega(\Delta_1) \rightarrow 2\omega(\Lambda_3)$. As the temperature is raised, the asymmetry becomes more pronounced, until at the highest temperature (880 K) a shallow valley develops between the main resonance maximum and a subsidiary maximum on the high-frequency shoulder. At high temperatures, where three-phonon scattering processes become important, the structure of the spectral function depends critically on the detailed frequency dependence of Δ and Γ. Indeed, the minimum of the valley can be shown to correspond to a region in frequency space where $\Gamma(\omega)$ exhibits a maximum. We have, in fact, in this region $\Gamma(\omega) \gg \Gamma'(\omega) \sim 0$ and $\Delta(\omega) \sim 0$ so that $\mathrm{Im}G(\omega) \sim 1/\Gamma(\omega)$ and the spectral function directly mirrors the ω dependence of Γ. This type of structure is illustrated even more vividly in Fig. 3(c) for the longitudinal (0.15, 0.15, 0.15) mode. In this case the resonance is perfectly Lorentzian at room temperature but develops significant structure at higher temperatures, this structure being characterized by twin peaks separated by a deep minimum. Here again the minimum corresponds to a maximum in $\Gamma(\omega)$. A further interesting feature of the (0.15, 0.15, 0.15) structure is the fact that between 700 and 880 K the maximum of the resonance shifts from the left-hand peak to the right-hand peak; this effect becomes even more pronounced for $T > 880$ K. The same effect can be seen in the frequency plot of the (0.9, 0, 0) phonon. What was merely a shoulder on the low-frequency side of the resonance at 700 K becomes the actual maximum at 880 K. Two other representative phonons, the (0.5, 0.5, 0.5) and (0.5, 0.5, 0) longitudinal modes, exhibit broad shoulders on the high-frequency side.

For the phonons displayed in Figs. 3(a)–3(c), the accuracy with which the approximations of Eq. (2) predict the true position of the resonance maxima and the true half-width becomes increasingly poor as the temperature is raised. It is clear that as the structure of the resonance becomes more complex it becomes increasingly more difficult to unambiguously define the true half-width; this is especially true if the resonance develops a prominent shoulder at about half-maximum. Furthermore, the identification of the renormalized phonon frequency is not itself unambiguous, especially if the true maximum of the resonance shifts discontinuously as for the (0.9, 0, 0) and (0.15, 0.15, 0.15) phonons.

ACKNOWLEDGMENTS

One of the authors (N. S. G.) wishes to thank W. J. Brya for useful discussions.

*Work supported by the U. S. Atomic Energy Commission.

[1]T. R. Koehler, N. S. Gillis, and Duane C. Wallace, Phys. Rev. B 1, 4521 (1970). Hereafter referred to as I.

[2]K. E. Larsson, U. Dahlborg, and S. Holmryd, Arkiv Fysik 17, 369 (1960).

[3]R. Orbach and L. A. Vredevoe, Physics 1, 91 (1964).

PHYSICAL REVIEW B VOLUME 3, NUMBER 10 15 MAY 1971

Transient Space-Charge-Limited Currents in Photoconductor-Dielectric Structures: A Comment

I. P. Batra, B. H. Schechtman, and H. Seki
IBM Research Laboratory, San Jose, California 95114
(Received 21 December 1970)

The calculation presented in an earlier paper is refined to include closed-form solutions for integrals of the exponential integral that were treated numerically in the original work. This allows us to demonstrate the equivalence of our results to those of Many and Rakavy for the limiting case of direct electrode contact to the photoconductor (no dielectric present).

In a recent paper[1] we presented the theory for transient space-charge-limited currents in photoconductor-dielectric structures. The structure was characterized by a parameter α which depended upon the relative thicknesses and dielectric constants of the two regions. It was shown that in one special limiting case ($\alpha = 1$) our general theory reproduced the results for the direct contact (no dielectric) configuration discussed by Many and Rakavy.[2] The equivalence of the two treatments was completely demonstrated, with the exception (as noted in Ref. 1) of the flow-line equation in zone II [Eq. (3.45) of Ref. 1] and consequently the equation [Eq. (3.46) of Ref. 1] which determined t_2, the time at which zone II ends. In our paper[1] we were unable to show the mathematical equivalence of these equations and